Pharm Res (2010) 27:2317–2329
DOI 10.1007/s11095-010-0091-0

RESEARCH PAPER

Temozolomide Delivery to Tumor Cells by a Multifunctional Nano Vehicle Based on Poly(β-L-malic acid)

Rameshwar Patil • José Portilla-Arias • Hui Ding • Satoshi Inoue • Bindu Konda • Jinwei Hu • Kolja A. Wawrowsky • Paul K. Shin • Keith L. Black • Eggehard Holler • Julia Y. Ljubimova

Received: 9 December 2009 / Accepted: 9 February 2010 / Published online: 13 April 2010

ABSTRACT

Purpose Temozolomide (TMZ) is a pro-drug releasing a DNA alkylating agent that is the most effective drug to treat glial tumors when combined with radiation. TMZ is toxic, and therapeutic dosages are limited by severe side effects. Targeted delivery is thus needed to improve efficiency and reduce non-tumor tissue toxicity.

Methods Multifunctional targetable nanoconjugates of TMZ hydrazide were synthesized using poly(β-L-malic acid) platform, which contained a targeting monoclonal antibody to transferrin receptor (TfR), trileucine (LLL), for pH-dependent endosomal membrane disruption, and PEG for protection.

Results The water-soluble TMZ nanoconjugates had hydrodynamic diameters in the range of 6.5 to 14.8 nm and ζ potentials in the range of −6.3 to −17.7 mV. Fifty percent degradation in human plasma was observed in 40 h at 37°C. TMZ conjugated with polymer had a half-life of 5–7 h, compared with 1.8 h for free TMZ. The strongest reduction of human brain and breast cancer cell viability was obtained by versions of TMZ nanoconjugates containing LLL and anti-TfR antibody. TMZ-resistant cancer cell lines were sensitive to TMZ nanoconjugate treatment.

Conclusions TMZ-polymer nanoconjugates entered the tumor cells by receptor-mediated endocytosis, effectively reduced cancer cell viability, and can potentially be used for targeted tumor treatment.

KEY WORDS anti-TfR mAb · nanoconjugate · pH-dependent membrane disruption · polymalic acid · targeted drug delivery · temozolomide

ABBREVIATIONS

TMZ	temozolomide
TMZH	temozolomide hydrazide
PMLA	Poly(β-L-malic acid)
HuTfR	anti-human transferrin receptor
mAb	monoclonal antibody
LOEt	L-leucine ethyl ester
LLL	L-leucine tripeptide
Alex680	Alexa Fluor® 680 C2 maleimide

Nanoconjugates are abbreviated as shown in Charts 3 and 4

R. Patil • J. Portilla-Arias • H. Ding • S. Inoue • B. Konda • J. Hu • K. L. Black • E. Holler • J. Y. Ljubimova (✉)
Department of Neurosurgery Cedars-Sinai Medical Center
8631 W. Third Street, Suite 800E
Los Angeles, California 90048, USA
e-mail: ljubimovaj@cshs.org

K. A. Wawrowsky
Department of Medicine Cedars-Sinai Medical Center
Los Angeles, California, USA

P. K. Shin
Department of Chemistry and Biochemistry
California State University
Northridge, California, USA

E. Holler
Institut für Biophysik und Physikalische Biochemie der Universität Regensburg
Regensburg, Germany

INTRODUCTION

Malignant gliomas are the most common (60–70%) of all CNS/brain tumors. Annually, there are approximately five cases of malignant gliomas per 100,000 people, and over 14,000 new cases are diagnosed each year in the United States (1,2). Surgery remains the standard therapy for primary brain tumors. Although surgery may be combined with radiation therapy and/or followed with chemotherapy

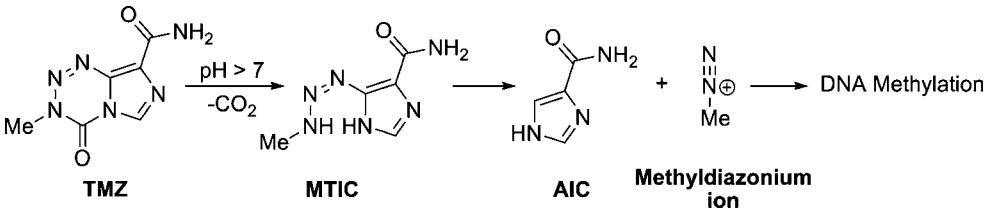

Chart 1 pH-dependent conversion of TMZ to metabolites, 5-(3-methyltriazen-1-yl)imidazole-4-carboxamide (MTIC), 4-amino-5-imidazole-carboxamide (AIC), methyldiazonium ion and DNA methylation (6).

to destroy remaining cancer cells, patients still have a poor survival (3–5). In recent years, Temozolomide (TMZ, Temodar®), a prodrug which undergoes spontaneous conversion to the active alkylating agent (Charts 1 and 2) has emerged as a potent chemotherapeutic agent (6). In combination with radiotherapy, it has been shown to substantially increase median survival compared with radiotherapy alone (7). However, TMZ has considerable toxicity, which prevents therapeutic dosage increase. Moreover, another limiting factor of TMZ treatment is tumor resistance to the drug (8–10).

Recently, efforts have been made to develop delivery systems for conventional chemotherapeutic drugs. Polymer-based delivery systems are less immunogenic than protein-based, e.g. viral vectors, and allow repetitive treatments without acute or chronic host immune response (11–14). Compared with most chemotherapeutic molecules, macromolecules offer several advantages, including tumor targeting, increased solubility, enhanced accumulation in solid tumors, decreased general toxicity, increased maximum tolerated doses, circumvention of multidrug resistance and enhanced apoptosis induction (15,16). Nanodrugs can selectively accumulate in tumor through a passive targeting mechanism known as enhanced permeability and retention (EPR) effect (17–19). Targeting efficiency is substantially enhanced by combining nanodrugs with specific antibodies that allow targeting by binding to antigens on the tumor cell surface (20–22).

To avoid systemic side effects by orally administered TMZ, targeting to brain tumor would be highly important. Recently, Brem (23) and Akbar (24) have administered a solid mixture of biodegradable polymer and TMZ directly into the brain tumor in animal models. The drug was progressively released during degradation of the embedding polymer material and significantly prolonged the survival time of experimental animals. These methods are invasive, and the drug is applied at the time of surgery. Moreover, gliomas are tumors with the ability to develop recurrences; thus, systemic and targeted delivery of TMZ would be a more beneficial treatment approach.

Following I.V. administration, we have delivered antisense oligonucleotides specifically to brain tumor using the targeted nanoconjugate delivery system, Polycefin (21). The nanoconjugate platform, poly(β-L-malic acid) (PMLA), is biodegradable, non-toxic and non-immunogenic, containing numerous pendant carboxyl groups suitable for the covalent attachment of prodrugs and other useful molecules. For the delivery into the cytoplasm of recipient glioma cells, we conjugated TMZ in its hydrazide form with PMLA along with anti-transferrin receptor (TfR) monoclonal antibody (mAb) for tumor targeting by receptor-mediated endocytosis (21) and pH-sensitive trileucine (LLL) for disruption of endosomal membranes.

The goal of this work was to engineer a TMZ nanoconjugate that could be specifically delivered into brain tumor cells and overcome drug resistance and general toxicity in order to improve treatment of brain cancer.

MATERIALS AND METHODS

Reagents Used

TMZ was purchased from AK Scientific, Inc. (Mountain View, CA, USA). TMZ hydrazide (TMZH) was synthesized from TMZ as described (25). Mouse anti-human TfR mAb RVS10 was purchased from Southern Biotech (Birmingham, AL, USA). PMLA (100 kDa; polydispersity 1.3; hydrodynamic diameter 6.6 nm; ζ potential −22.5 mV, pH 7.5 at 25°C) was obtained from culture broth of *Physarum polycephalum* as described (26). $mPEG_{5000}$-amine and maleimide-PEG_{3400}-maleimide were obtained from Laysan Bio, Inc. (Arab, AL, USA). NH_2-Leu-OEt (LOEt) and NH_2-Leu-Leu-Leu-OH (LLL) were purchased from Bachem Americas, Inc. (Torrance, CA, USA). Egg yolk and phosphatidylcholine were from Fluka (Buchs, Switzerland). 3-(2-Pyridyldithio)-propionate (PDP) was synthesized as described (27). Alexa Fluor® 680 C2 maleimide (Alex680) was from Invitrogen Corporation

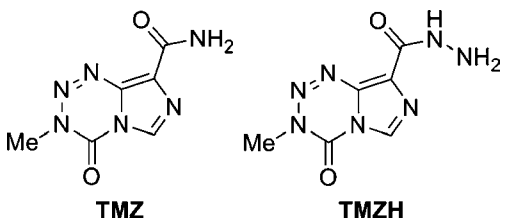

Chart 2 Temozolomide (TMZ) and temozolomide hydrazide (TMZH).

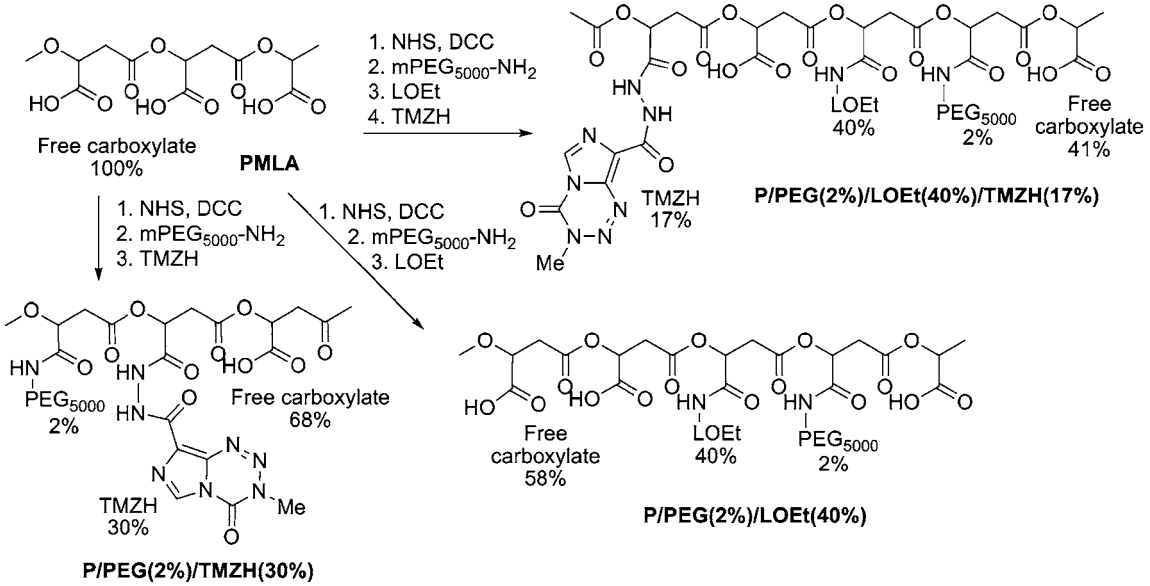

Chart 3 Synthetic strategy for LOEt conjugates containing TMZH.

(Carlsbad, CA, USA). Unless otherwise indicated, all chemicals and solvents of highest purity were purchased from Sigma-Aldrich (St. Louis, MO) USA.

Analytical Methods for Chemical Synthesis

The conjugation reaction of PMLA with PEG, TMZH, LLL and LOEt was followed by thin layer chromatography (TLC) on precoated silica gel 60 F254 aluminum sheets (Merck, Darmstadt, Germany) and visualization of spots by UV light and/or by ninhydrin staining. The concentration of free or conjugated TMZH was monitored by reading A_{328} and using known amounts of TMZ or TMZH standards. Size exclusion chromatography was performed on an Elite LaChrom analytical system with Diode Array Detector L 2455 (Hitachi, Pleasanton, CA, USA), and M_w was measured using BioSep-SEC-S 3000 (300×7.80 mm) (Phenomenex, Torrance, CA, USA) with 50 mM sodium phosphate buffer pH 6.8 and polystyrene sulfonates as molecular weight standards. Thiol residues attached to PMLA were assayed by the method of Ellman. Enzyme-linked immunosorbent assay (ELISA) was used to determine the functional activity of conjugated antibody using a Protein Detector™ ELISA Kit (KPL, Inc., Gaithersburg, MA, USA). Human TfR ectodomain used as antigen was obtained from Protein Expression Center, California Institute of Technology, Pasadena, USA.

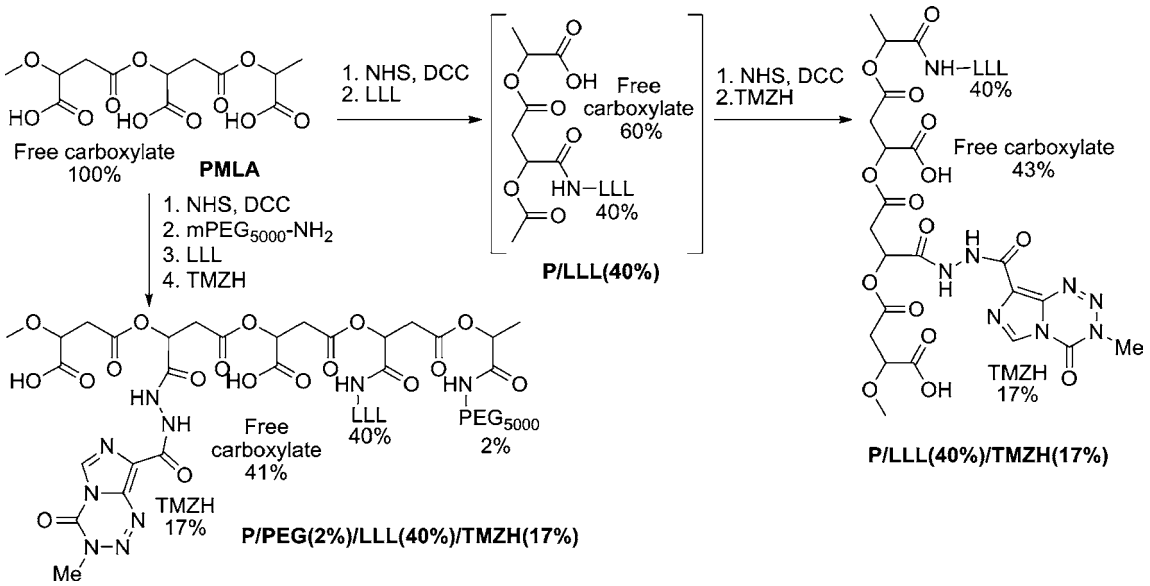

Chart 4 Synthetic strategy for LLL conjugates containing TMZH.

Syntheses of Nanoconjugates

A variety of conjugates were synthesized in order to examine the effect of each conjugated functional group on membrane disruption and cell viability. Two membrane-disrupting units were examined for their usefulness in endosome escape: LOEt and LLL. The synthetic strategies for the nanoconjugates containing the LOEt endosomal escape unit are summarized in Chart 3, and those containing LLL endosomal escape unit in Chart 4. Conjugates containing different amounts of TMZH were synthesized by analogous methods.

Conjugate P/PEG(2%)/TMZH(30%)

N-Hydroxysuccinimide (NHS) (1 mmol) and N,N′-dicyclohexylcarbodiimide DCC (1 mmol) dissolved in 2 ml of DMF were added consecutively to the solution of 116 mg of PMLA (1 mmol with regard to malyl units) dissolved in 1 ml of anhydrous acetone under vigorous stirring at room temperature (RT). The reaction mixture became turbid almost immediately upon addition of the NHS/DCC mixture, indicating the formation of dicyclohexylurea. After stirring at RT for 3 h to complete the activation of carboxyl groups, 0.02 mmol of $mPEG_{5000}$-NH_2 (in 0.5 ml of DMF, 2 Mol-% with regard to malyl units) was added followed by 0.02 mmol of triethylamine (TEA). After the reaction was completed according to TLC/ninhydrin test, the reaction mixture was filtered, and most of the solvent was removed by rotary evaporation. Next, 0.3 mmol of TMZH (15 mg/ml in DMF, 30 Mol-% with regard to malyl units) was added drop-wise at RT under stirring followed by 0.3 mmol of TEA. The reaction was complete within 2 h according to TLC (Rf=0.4 for TMZH; Rf=0 for the polymer conjugate; chloroform: methanol 9:1; visualization under UV and by ninhydrin). Addition of 5–6 ml 100 mM sodium phosphate buffer containing 150 mM NaCl (pH 6.0) to the reaction mixture was followed by 30 min stirring at RT. After centrifugation at 1500 × g for 10 min, the clear supernatant was passed over a Sephadex column (PD-10, GE Healthcare, Piscataway, NJ, USA) pre-equilibrated with deionized (DI) water. The product-containing fractions were collected, and conjugate P/PEG(2%)/TMZH(30%) was obtained after freeze drying.

Conjugate P/PEG(2%)/LOEt(40%)/TMZH(17%)

PMLA activation and conjugation of PEG followed the method described for conjugate P/PEG(2%)/TMZH (30%). A solution of LOEt hydrochloride (200 mM in DMF, 40 Mol-% with regard to malyl units) was added drop-wise at RT under stirring, followed by addition of 0.4 mmol of TEA. The reaction was complete after 2 h according to TLC (Rf=0 for the polymer conjugate, Rf= 0.67 for LOEt; n-butanol:acetic acid:water 4:2:2) and visualization of spots by ninhydrin. Next, 0.17 mmol of TMZH (15 mg/ml in DMF, 17 Mol-% with regard to malyl units) was added drop-wise under stirring at RT, followed by 0.17 mmol of TEA. After reaction completion in 2 h as judged by TLC (Rf=0.4 for TMZH; Rf=0 for the polymer conjugate; chloroform:methanol 9:1), UV and ninhydrin test, conjugate was dissolved in phosphate buffer, isolated as described for P/PEG(2%)/TMZH(30%), and freeze dried. To isolate the intermediate product P/PEG (2%)LOEt(40%), the same method for isolation was used, and the product was obtained after freeze drying.

Synthesis of Conjugate P-LLL(40%)/TMZH(17%)

PMLA activated at carboxyl groups was prepared as described for conjugate P/PEG(2%)/TMZH(30%). A solution of LLL, 0.4 mmol, 50 mg/ml in DMF (40 Mol-% with regard to malyl units) and TFA (125 Mol-% with regard to LLL, to dissolve the tripeptide) was added at RT. TEA (0.4 mmol in DMF, 1:25 v/v) was then added slowly over 30 min. After 2–3 h the reaction was complete by TLC (Rf= 0 for polymer conjugate; Rf=0.6 for LLL; n-butanol:acetic acid:water 4:2:2) and by ninhydrin test. Conjugate P/LLL (40%) was dissolved in phosphate buffer and isolated as described for conjugate P/PEG(2%)/TMZH(30%). In order to maximize TMZH loading, a second round of carboxyl activation was performed: A solution of NHS (0.217 mmol) and of DCC (0.217 mmol) in 1 ml of DMF were added consecutively to the solution of 56 mg of P/LLL(40%) (0.217 mmol of free acid groups) dissolved in 1 ml of anhydrous DMF under vigorous stirring at RT. After stirring for 3 h at RT, 0.037 mmol of TMZH (15 mg/ml in DMF, 17 mol% with regard to malyl units) was added drop-wise at RT, followed by 0.037 mmol of TEA. The reaction mixture was stirred at RT for 3 h, and the conjugate was isolated as described for P/PEG(2%)/TMZH(30%).

Synthesis of P/PEG(2%)/LLL(40%)/TMZH(17%)/ MEA(3%)

This conjugate was used for the conjugation of antibody. The conjugate not containing 2-MEA was synthesized in the absence of this reagent.

PMLA activated at carboxyl groups was prepared as described for conjugate P/PEG(2%)/TMZH(30%). A solution of LLL, 0.4 mmol, in DMF 50 mg/ml (40 Mol-% with regard to malyl units) and TFA (125 Mol-% with regard to LLL) was added drop-wise to dissolve the tripeptide at RT. TEA 0.4 mmol in DMF (1:25 v/v) was then added slowly over 30 min. The reaction was complete after 2–3 h by TLC (Rf=0 for polymer conjugate; Rf=0.6 for LLL; n-butanol:acetic acid:water 4:2:2) and by ninhydrin test. Next, TMZH (15 mg/ml in DMF, 17 Mol-% or

optionally 30 Mol-% with regard to malyl units) was added drop-wise under stirring at RT followed by equivalent amount of TEA. After reaction completion in 2–3 h, as judged by TLC (Rf=0.4 for TMZH; Rf=0 for the polymer conjugate; chloroform:methanol 9:1), UV, and ninhydrin test, 0.05 mmol of 2-MEA in DMF (100 μl, 5 Mol-% with regard to malyl units) was added to the reaction mixture. After reaction completion in 30–40 min (TLC and ninhydrin test), conjugate was dissolved in phosphate buffer and isolated as described for conjugate P/PEG(2%)/TMZH(30%).

Conjugate P/PEG(2%)/LLL(40%)/TMZH(17%)/HuTfR mAb(0.25%)

A solution of anti-human TfR mAb (HuTfR)/PEG_{3400}/maleimide (2 mg/ml) synthesized as described (28) and dissolved in 100 mM sodium phosphate buffer containing 150 mM NaCl (pH 6.0) was added drop-wise at RT to a solution of P/PEG(2%)/LOEt(40%)/TMZH(17%)/MEA (3%) at 2 mg/ml in the same buffer. After stirring overnight at 4°C, remaining free –SH groups were blocked by excess PDP (50 mg/ml in DMF) by stirring for 30 min at RT. The product was concentrated over a centrifuge membrane filter Vivaspin 20, cutoff 30 kDa, 20 ml at 1500 × g (Sartorius Stedim Biotech, Concord, CA, USA), and the final volume was adjusted to 2 ml before purification over Sephadex G-75 pre-equilibrated with buffer, 100 mM sodium phosphate, 150 mM NaCl, pH 6.8. Product-containing fractions were isolated, combined and concentrated via membrane filtration. Similar methods were used to synthesize other antibody-containing conjugates.

Fluorescent Labeling of Conjugates

Alex680 dissolved in DMF at 1 mg/ml was added to the solution of desired conjugates (2 mg/ml) in 100 mM sodium phosphate buffer with 150 mM NaCl, pH 5.5. The reaction mixture was stirred at RT for 1 h and passed over Sephadex G-75 pre-equilibrated with 100 mM sodium phosphate buffer, 150 mM NaCl, pH 6.8. The product was concentrated via membrane filtration. For the antibody-containing conjugates, Alex680 labeling was performed before blocking of excess free thiol groups by PDP.

Calculation of Molecular Weights of Nanoconjugates

Molecular weights of nanoconjugates were calculated as shown for conjugate P/PEG(2%)/LLL(40%)/TMZH(17%) as an example: 100% malic acid residues (FW 116)=862 monomers of PMLA (M_w=100 kDa). M_w fraction of malic acid with free -COOH (FW116) is 41%=353.4×116 Da: 41.0 kDa. Fraction-conjugated malic acid (FW 99) is 59%=508.6×99 Da: 50.3 kDa. Fraction $mPEG_{5000}$ (FW 5000) is 2%=17.2×5000 Da: 86.2 kDa. Fraction LLL (FW 357.5) is 40%=344.8×357.5 Da: 123.3 kDa. Fraction TMZH (FW 210.63) is 17%=146.5×210.63: 30.8 kDa. Total estimated average Mw of conjugate is 332 kDa.

Hydrodynamic Diameter and Zeta Potential

Synthesized conjugates were characterized with respect to their size and ζ potential using Zetasizer Nano ZS90 (Malvern Instruments, Malvern, UK). The size was calculated on the basis of noninvasive back-scattering (NIBS) measurements using the Stokes-Einstein equation, $d(H)=kT/3\pi\eta D$. $d(H)$ is the hydrodynamic diameter, D translational diffusion coefficient, k Boltzmann's constant, T absolute temperature, and η viscosity. The diameter that is measured in DLS (Dynamic Light Scattering) refers to the particle diffusion within a fluid and is referred to as the hydrodynamic diameter corresponding to the diameter of a sphere that has the same translational diffusion coefficient as the particle. The ζ potential was calculated from the electrophoretic mobility based on the Helmholtz-Smoluchowski formula, using electrophoresis M3-PALS (29,30). All calculations were carried out by the Zetasizer 6.0 software. For the particle size measurements at 25°C, the solutions were prepared in PBS at a concentration of 2 mg/ml, filtered through a 0.2 μm pore membrane. For the measurement of the ζ potential, the concentration of the sample dissolved in water containing 10 mM NaCl was 2 mg/ml, and the voltage applied was 150 V. All the conjugate solutions were prepared immediately before analysis at 25°C. Data represent the mean± standard deviation obtained for three measurements.

Liposome Leakage Assay

Fluorescent assay for calcein release from loaded phosphatidylcholine/cholesterol liposomes (31) purified over Sephadex G-50 was used to determine leakage activity of synthesized polymer conjugates. To assess leakage at different pH values, nanoconjugates were serially diluted in 50 μl buffer containing appropriate mixtures of 137 mM HEPES, pH 7.4 and 137 mM citrate, pH 5.0. Triplicate samples were mixed with 50 μl liposome suspensions in 5 mM HEPES buffer, 150 mM NaCl, pH 7.4 (final lipid concentration 160 μM). After 1 h at RT, fluorescence was read by an ELISA reader at 485 nm excitation and 535 nm emission wavelengths. Triton X-100, 0.25% (v/v), was used as a reference for 100% leakage.

Conjugate Degradation Study

The degradation of nanoconjugates in human plasma was carried out at 37°C with a polymer concentration of 1 mg/ml. The sample vials were sealed to avoid evaporation and stored at 37°C in an incubator. For the isolation from the

plasma, aliquots of 1 ml were extracted with 5 ml of chloroform/ethyl acetate (1:1 v/v). The copolyester contained in the organic phase was dried and re-dissolved in PBS buffer. Size reduction due to degradation was followed by measurement of the hydrodynamic diameter in Zetasizer or of the molecular weight by SEC-HPLC. Sample preparation with the polymers of known M_w was used to verify that the isolation method had no effect on molecular weights. Degradation in PBS (pH 7.4) was followed at a concentration of 1 mg/ml for each copolymer. The change in size of the nanoconjugate either by SEC-HPLC or hydrodynamic diameter (Zetasizer) was measured as a function of degradation time. Molecular weights and hydrodynamic diameter (t) were plotted as a function of degradation time with reference of these properties at zero incubation time.

Cell Viability

Primary glioma cell lines U87MG and T98G, and invasive breast carcinoma cell lines MDA-MB-231 and MDA-MB-468 were obtained from American Type Culture Collection (ATCC, Manassas, VA, USA). U87MG and T98G cells were cultured in minimum essential media (MEM) supplemented with 10% fetal bovine serum, 1% MEM NEAA, 1 mM sodium pyruvate and 2 mM L-glutamine. For MDA-MB-231 and MDA-MB-468, Leibovitz's L-15 medium with 10% fetal bovine serum was used. Cells were seeded at 10^3 per well (0.1 ml) in 96-well flat-bottomed plates and incubated overnight at 37°C in humid atmosphere with 5% CO_2 (MDA-MB-231 and MDA-MB-468 were incubated without CO_2). After exposure to synthesized conjugates for 24 h, medium was replaced every 48 h. Cell viability was measured on day 5 for T98G and day 7 for the rest of the cell lines using the CellTiter 96 Aqueous One Solution Cell Proliferation Assay kit (Cat. No.PR-G3580; Promega, Madison, WI, USA). Yellow [3-(4,5-dimethylthiazol-2-yl)-5-(3-carboxymethoxyphenyl)-2-(4-sulfophenyl)-2H-tetrazolium, inner salt] (MTS) is bioreduced by cells into formazan that is soluble in the tissue culture medium. The absorbance reading at 490 nm from the 96-well plates is directly proportional to the number of living cells (32). The viability of the untreated cells was taken as 100%. The results shown are the means±standard deviation of three independent measurements. Data were analyzed by statistical software GraphPad Prism 3.0.

Confocal Microscopy

1×10^5 U87MG cells were seeded on Lab-Tek™ chamber slides (Thermo Fisher Scientific, Rochester, NY, USA) for 24 h. The cells were washed once with serum-free media and incubated with Alex680 fluorescently labeled conjugates in 500 µl serum-free media at 50 µg/ml for P/PEG(2%)/LLL(40%)TMZH(17%)/Alex680(1%) and at 100 µg/ml for P/PEG(2%)/LLL(40%)TMZH(17%)/HuTfR mAb(0.25%)/Alex680(1%). After 1 h incubation at 37°C in humid atmosphere with 5% CO_2, the cells were washed three times with PBS and finally incubated in fresh media with serum for live confocal imaging in a TCS SP spectral scanner (Leica Microsystems, Mannheim, Germany). Image stacks of 246 by 246 µm in size and 7.5 µm in depth of live U87MG glioma cells were acquired with a HCX PL APO CS 63.0× 1.20 lens. Live cells were placed on chamber slides maintaining 37°C temperature, humidity and 5% CO_2 by a separate lens and chamber heating system. The spectral settings were optimized for Alex680, excitation 670 nm and emission 685–750 nm. The images were processed by ImageJ 1.41o software from NIH.

RESULTS

Nanoconjugate Syntheses

The multi-component drug delivery system schematically presented in Fig. 1 was synthesized with PMLA as the platform and prodrug TMZ in its hydrazide form, H_2N-Leu-Leu-LeuOH (LLL) or NH_2-LeuOEt (LOEt) for disruption of endosomal membrane, antibodies for targeting, and PEG against resorption and enzyme degradation. The first part of the conjugation included the chemical activation of the PMLA pendant carboxyl groups forming the NHS-ester and subsequently the nucleophilic replacement by forming stable amide bonds. Conjugation of antibodies via thioether bond formation followed in the second part. Because of the PMLA chain length inhomogeneity, an excess of mAb was chosen in order to increase the likelihood that at least one molecule was conjugated with each polymer chain. The amount of 40% of carboxyl groups conjugated with LLL for most efficient membrane disruption activity limited the amount of TMZH conjugation to 17%. In order to increase the amount of TMZH loading, carboxyl activation was repeated after conjugation with LLL before conjugation with TMZH. Obtained nano-

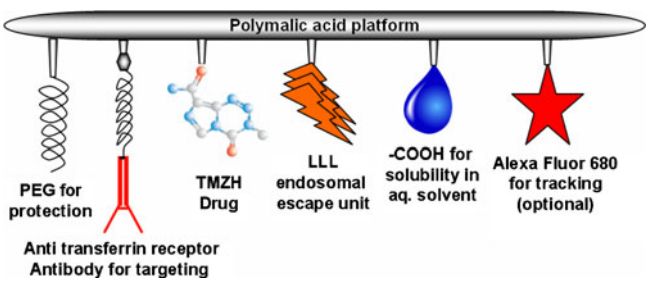

Fig. 1 Schematic presentation of the drug delivery system.

Table I. Physicochemical Properties of the Conjugates and Half-Lives of TMZ

Conjugates	Hydrodynamic diameter(nm)[a]	Zeta potential (mV)[b]	Half-life of TMZ (h)[c]
TMZ	n.d.	n.d.	1.80 (±0.1)[d]
TMZH	n.d.	n.d.	1.98 (±0.1)
PMLA	6.6 (±0.1)	−22.9 (±1.7)	n.d.
P/PEG(2%)/TMZH(30%)[e]	7.8 (±0.4)	−16.1 (±1.2)	7.10 (±0.2)
P/PEG(2%)/LOEt(40%)/TMZH(17%)	8.5 (±0.4)	−6.7 (±0.2)	4.92 (±0.3)
P/PEG(2%)/LLL(40%)/TMZH(17%)	6.9 (±1.3)	−11.5 (±1.8)	6.25 (±0.2)
P/LLL(40%)/TMZH(17%)	6.5 (±0.2)	−17.7 (±2.1)	7.34 (±0.2)
P/PEG(2%)/LLL(40%)/TMZH(17%))/HuTfR mAb(0.25%)	14.8 (±2.1)	−6.3 (±1.7)	n.d.

[a] Hydrodynamic diameter at 25°C measured in PBS at a concentration of 2 mg/ml

[b] ζ potential at 25°C in aqueous solution of 10 mM NaCl at 150 V

[c] Half-life measured at physiological pH in PBS at 37°C

[d] Mean values and S.D. for three independent measurements

[e] Percentage refers to total number (100%) of pendant carboxyl groups in unsubstituted PMLA; n.d., not done.

conjugates of higher than 17% TMZH were, however, found insoluble in aqueous buffer. Care was taken to avoid neutral or alkaline conditions as well as elevated temperatures (>22°C) in order to keep hydrolytic degradation of TMZ at a minimum. Freeze-dried intermediates and products could be stored at −20°C for several months without measurable loss in chemical or physiological reactivity.

Purity and Physicochemical Characterization

Products were highly soluble in aqueous solution without forming precipitates as judged by SEC-HPLC and Zetasizer. Preparations were tested for small molecular weight impurities by TLC and ninhydrin reaction. On this basis of SEC-HPLC results (using multiple wavelengths for scanning) and hydrodynamic diameter scanning, the investigated conjugates were pure, i.e. consisting of single compounds. The amount of TMZH in the conjugate preparations was validated by UV absorbance at 328 nm using known amounts of free TMZH as standards. By ^{1}H NMR analysis using integration of methyl group signals of TMZH and of PMLA protons, the TMZH contents were analyzed. TMZ contents by NMR and UV measurement were the same within 3% deviation measured for conjugate P/PEG(2%)/TMZH(30%). Conjugates had characteristic values of hydrodynamic diameters and zeta potentials (Table I). Free PMLA and P/LLL(40%)/TMZH(17%) had the smallest hydrodynamic diameter, whereas additionally conjugated PEG_{5000} increased the diameter by about 2 nm and mAb by about 8 nm. The value of ζ potential can be used to differentiate between PMLA, −22.9 mV, and nanoconjugates with neutral ligands like TMZH, LOEt (e.g., −7 mV for P/PEG(2%)/LOEt(40%)/TMZH(17%)) and conjugates with charged ligands like LLL (instead of LOEt) (e.g., −11.5 mV for P/PEG(2%)/LLL(40%)/TMZH(17%)) (Table I). Conjugates were also distinguished by other properties, e.g., capability for liposome leakage. As shown in Fig. 2, the conjugate P/PEG(2%)LLL(40%)/TMZH(17%) was pH-sensitive, whereas the conjugate P/LLL(40%)/TMZH(17%) was not. Another property was the effect on U87MG and

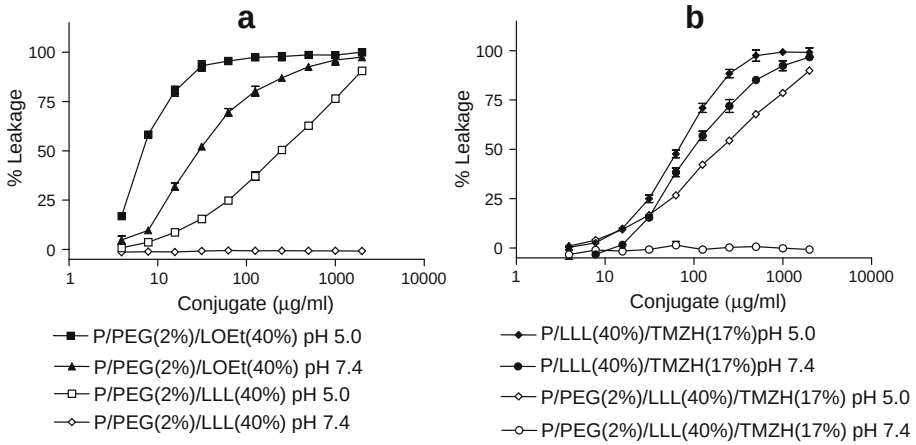

Fig. 2 Liposomal leakage assay: a) Liposome leakage of P/LOEt and P/LLL conjugates, b) Liposome leakage of P/LLL/TMZH and P/PEG/LLL/TMZH conjugates. Percentage refers to ratio of pendant –COOH conjugated (total PMLA pendant –COOH is 100%). % Leakage compared to complete leakage in the presence of 0.25% (v/v) Triton X-100.

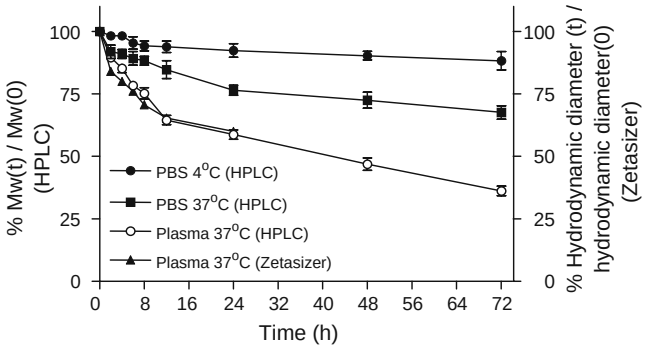

Fig. 3 Nanoconjugate degradation in PBS and human plasma. Degradation of conjugate P/LLL(40%)TMZH(17%) in PBS and human plasma at 4°C and 37°C studied by relative changes in molecular size indicated by column retention times (% molecular weights) of SEC-HPLC and hydrodynamic diameter (t) measured by Zetasizer. 100% refers to the size at time zero.

MDA-MB-468 cell viability. It was more affected by the conjugate P/LLL(40%)/TMZH(17%) (Fig. 4) than by P/PEG(2%)LLL(40%)/TMZH(17%) (Fig. 6).

Half-Life of Free and Conjugated TMZH

TMZ is a prodrug and undergoes spontaneous conversion to the active alkylating agent at neutral or alkaline pH. Half-lives were measured at physiological pH 7.4 in PBS and summarized in Table I. The decomposition of free and conjugated TMZH by hydrolytic ring opening (Chart 1) was a first-order reaction for free TMZ or TMZH and conjugated TMZH (data not shown). The half-life was 1.80 ± 0.1 h for TMZ and 1.98 ± 0.1 h for TMZH. Half-life was significantly enhanced, about 3–4 times, after conjugation with the polymer. For example, TMZ had a half-life of 7.34 ± 0.2 h for conjugate P/LLL(40%)/TMZH(17%) and 7.10 ± 0.2 h for P/PEG(2%)/TMZH(30%) (Table I). Similar data have been reported for TMZ conjugated with small carbon chains (6). No detectable decomposition was observed during 24 h at pH 5.0 at RT.

Stability and Degradation Measured by Size

Degradation of synthesized nanoconjugates was measured by SEC-HPLC and Zetasizer in terms of molecular weight and hydrodynamic diameter, respectively (data not shown). In PBS at 4°C, all synthesized nanoconjugates were stable, maintaining over 85% of original M_w/size for more than 72 h. However, at temperatures 25°C and especially at 37°C, substantial degradation was observed, and M_w/size was reduced to 50% after 24–72 h in PBS. In human plasma at 37°C, conjugates degraded more rapidly compared with degradation in PBS, and M_w/size was reduced by 50% after 12–36 h. As an example, degradation of conjugate P-LLL (40%)/TMZH(17%) is shown in Fig. 3.

Membrane Destabilization

As an uncharged prodrug, TMZ can passively permeate the cells, where it is ultimately activated to the nucleic acid methylating methyldiazonium cation (33). Targeting of glioma cells by conjugated mAb would involve binding of

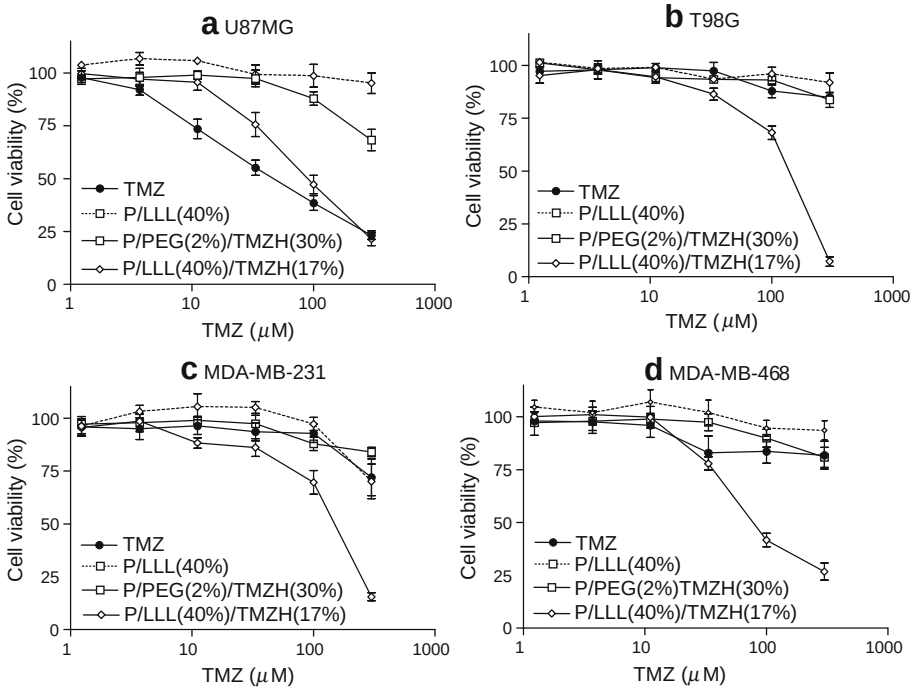

Fig. 4 Cell viability of nanoconjugate with LLL: Effects on cell viability of TMZ, P/LLL(40%), P/PEG(2%)/TMZH(30%) and P/LLL(40%)/TMZH(17%) on a) U87MG, b) T98G, c) MDA-MB-231 and d) MDA-MB-468 cells. Nanoconjugate P/LLL(40%) without drug was used as a control for the conjugate P/LLL(40%)/TMZH(17%) with drug and contains equivalent amount of polymer backbone. Nanoconjugate P/PEG(2%)/TMZH(30%) even with high loading of TMZH but without LLL endosome escape unit was only marginally effective. P/LLL(40%)/TMZH(17%) was the most effective nanoconjugate.

the nanoconjugate delivery vehicle to overexpressed TfR and subsequent internalization into the endosomal system. In order to deliver the desired drug into the cytoplasm, disruption of the endosomal membrane would be essential. By systematic structure variation using PMLA as nanoplatform and membranes of artificial liposomes, we have found LOEt and LLL substituting 40% of pendant PMLA carboxyates of the platform to be excellent candidates for endosomal membrane disruption (Fig. 2). Whereas the LLL unit was active only at pH 6–5.0 (Fig. 2a), resembling pH of late endosomes and lysosomes, the membrane disruption activity of the LOEt unit was pH-independent. The pH dependence for LLL was referred to the ionization of the tripeptide carboxyl group. The pK_a that governs ionization was shifted by conjugation with PMLA towards the neutral pH region due to the hydrophobic shielding by the multiple conjugated leucine side chains (Ding *et al.* "Poly(β-l-malic acid) with pendent leu-leu-leu-OH for endosome-routed cytoplasmic delivery." 14th International Symposium on Recent Advances in Drug Delivery Systems, Salt Lake City, 2009, Abstract #91). Fig. 2 shows examples of liposome leakage caused by membrane disruption in the absence and presence of TMZH. LOEt wasthe more effective membrane-disrupting agent (Fig. 2a). The loading by TMZH slightly increased the liposome leakage activity by LOEt and LLL units, but did not abolish the pH dependence for conjugate P/PEG(2%)LLL(40%)/TMZH (17%) (Fig. 2b). When TMZH was conjugated as in P/LLL (40%)/TMZH(17%), the leakage activity was improved, and the pH sensitivity disappeared (Fig. 2b). Most likely, this change was attributed to conjugation of TMZH with LLL-COOH residues, thus eliminating the carboxylates that before gave rise to the observed pH dependence.

Cell Viability Study

Effects of the nanoconjugates on cell viability were measured in order to investigate the influence of the delivery system on the TMZH prodrug activity and to test for cytotoxic activities of the delivery system itself in the absence of the prodrug. Results were compared with those for free TMZ and TMZH in a dose-dependent manner. P/PEG(2%)/TMZH(30%) had no significant effect on viability compared with free TMZ in the case of human glioma cell line U87MG (Fig. 4a), and it was ineffective on T98G, MDA-MB-231 and MDA-MB-468 cell lines (Fig. 4b–d). Conjugation of membrane disruption unit had pronounced effects on cell viability. Introduction of LOEt as a membrane disruption unit seemed to decrease cell viability significantly (Fig. 5); however, the decrease was apparently due to the nanoconjugate P/PEG(2%)/LOEt(40%) carrier itself and not by conjugated TMZH. As LOEt negatively affected cell viability in the observed concentration range, conjugates with this endosomal escape unit were not further considered. Importantly, introduction of LLL in the conjugate P/LLL(40%)/TMZH(17%) significantly decreased cell viability of all four cell cultures, gliomas U87MG and T98G, and breast cancer cell lines MDA-MB-231 and MDA-MB-468. In the same assay, free TMZ was inactive in all lines except U87MG. Conjugate P/LLL(40%) as a control had little or no effect on cell viability due to the absence of the prodrug (Fig. 4), and this was not changed by the addition of PEG_{5000} (data not shown). The effect of coupling anti-TfR mAb to the nanoconjugate is shown in Fig. 6a. Whereas free TMZ had a stronger effect on U87MG cells than the nanoconjugates, these showed an increasing potency in the order P/PEG(2%)/LLL(40%)/TMZH(17%)/IgG(0.25%)<P/PEG(2%)/LLL(40%)/TMZH(17%) < P/PEG(2%)/LLL(40%)/TMZH(17%)/HuTfR mAb(0.25%)< TMZ. In contrast, with the cell line MDA-MB-468, free TMZ was ineffective at all concentrations below 130 μM, whereas conjugates P/PEG(2%)/LLL(40%)/TMZH(17%)/IgG (0.25%), P/PEG(2%)/LLL(40%)/TMZH(17%), P/PEG (2%)/LLL(40%)/TMZH(17%)/HuTfR mAb(0.25%) showed significant reduction in viability and were almost equally effective.

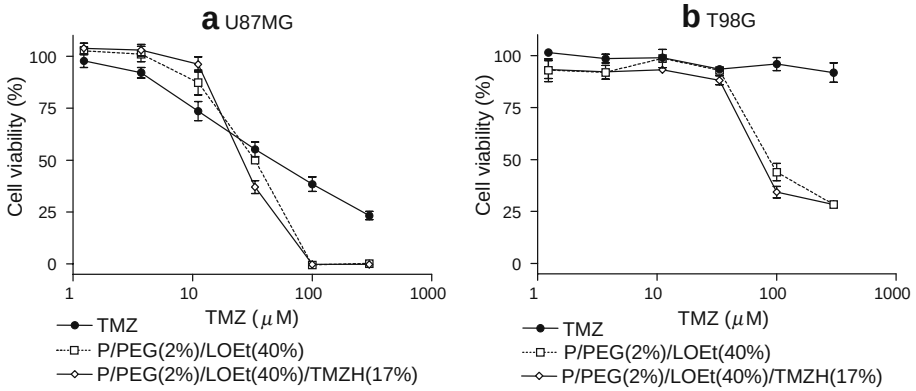

Fig. 5 Cell viability of nanoconjugate with LOEt: Effects on cell viability of TMZ, P/PEG(2%)/LOEt (40%) and P/PEG(2%)/LOEt (40%)/TMZH(17%) on **a**) U87MG and **b**) T98G cells. Nanoconjugate P/PEG(2%)/LOEt (40%) without drug was used as a control for the conjugate P/PEG (2%)/LOEt(40%)/TMZH(17%) with drug and contains equivalent amount of polymer backbone.

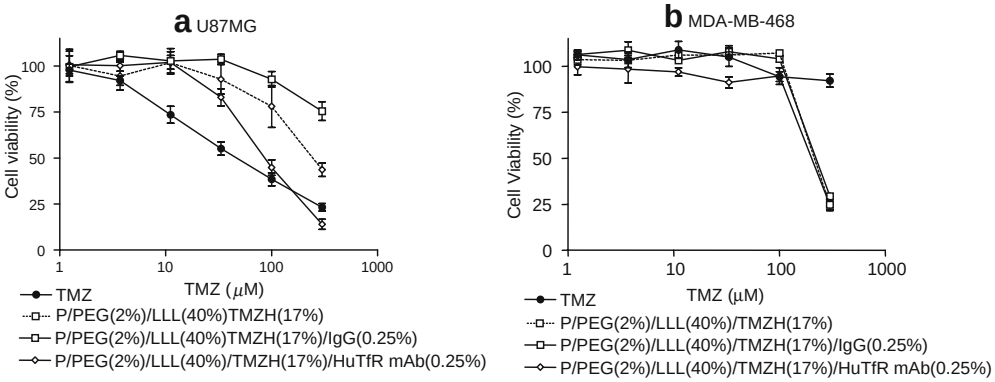

Fig. 6 Cell viability of LLL nanoconjugates with antibody: Effects on cell viability of TMZ, P/PEG (2%)/LLL(40%)/TMZH(17%), P/PEG(2%)/LLL(40%)/TMZH (17%)/IgG(0.25%), P/PEG(2%)/LLL(40%)/TMZH(17%)/HuTfR mAb(0.25%) on a) U87MG and b) MDA-MB 468 cells. Conjugation of HuTfR mAb increased the activity of drug on U87MG cell line, whereas no such effect was observed on MDA-MB-468.

Confocal Microscopy

The uptake of nanoconjugates was imaged by confocal microscopy following the appearance of fluorescence inside live human glioma U87MG cells (Fig. 7). Uptake into vesicles was observed for both conjugates P/PEG(2%)/LLL(40%)/TMZH (17%) and P/PEG(2%)/LLL(40%)/TMZH(17%)/HuTfR mAb(0.25%) labeled with Alex680. At a fixed instrument setting, the intensity and the number of vesicles were higher for the actively targeting conjugate with TfR mAb than for the conjugate lacking the antibody. It can be concluded that the nanodrugs were internalized most likely by receptor-mediated endocytosis and possibly also by pinocytotic pathways.

DISCUSSION

Orally applied TMZ to treat human gliomas would distribute all over the entire body indiscriminately. After penetration of the lipophilic prodrug through membranes into the cytoplasm of the cells, it will be activated by the hydrolytic mechanism described in Chart 1. The active drug is then ready to methylate proteins and especially DNA, guanine at N7 position, followed by methylation of adenine at the O3 position and of guanine at the O6 position (33). Failure of repair will drive these cells into apoptosis. Hydrolytic activation of the prodrug at sites other than the cytoplasm is inefficient due to the fact that the cationic methyl diazonium like any other charged molecule cannot passively penetrate membranes.

We have succeeded to conjugate TMZ via the hydrazide bond to the highly negatively charged PMLA that renders the prodrug no longer diffusible through membranes. More importantly, the conjugate would render EPR effect *in vivo* and warrant more tumor selective delivery and prolonged plasma half-life due to the macromolecular nature. As it reaches to the tumor cells with TfR, the conjugate will be internalized as discussed (34,35). As a consequence, the

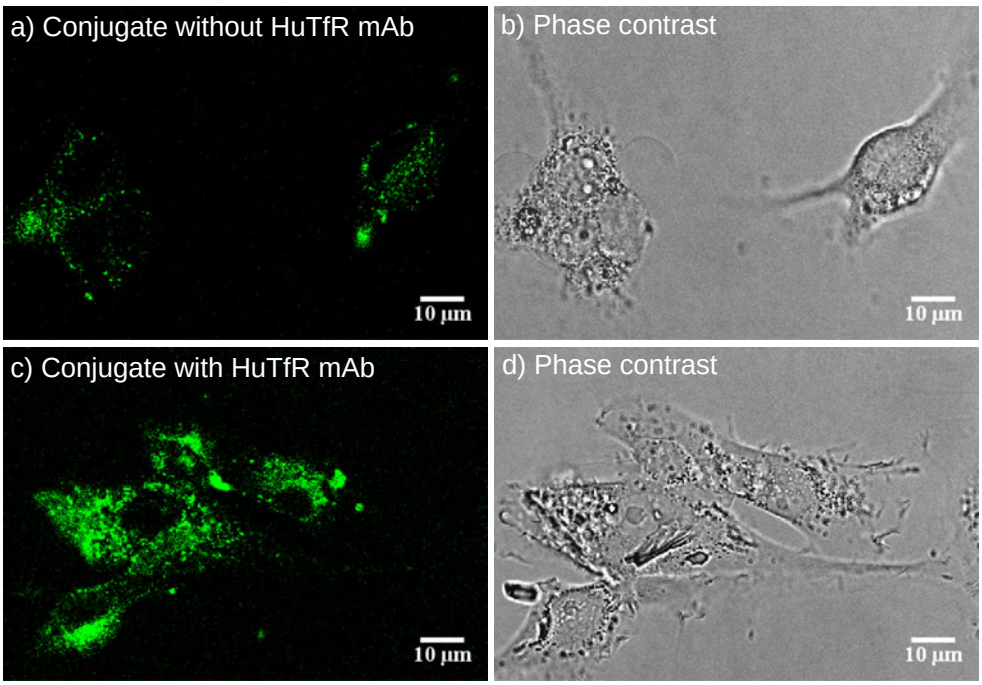

Fig. 7 Drug internalization into cultured human glioma U87MG cells by confocal microscopy: **a**) 1 h incubation with fluorescently labeled conjugate P/PEG(2%)/LLL (40%)TMZH(17%)/Alx680(1%). The location of conjugate is indicated by green fluorescence; **b**) phase contrast; **c**) 1 h incubation with fluorescently labeled conjugate P/PEG(2%)/LLL(40%)TMZH (17%)/HuTfR mAb(0.25%)/Alx680(1%). The location of conjugate is indicated by green fluorescence; **d**) phase contrast.

active methyl diazonium cation can only be generated from the nanodrug more selectively in tumor tissue. Free passive diffusion of the PMLA conjugate into recipient cells is highly unlikely because of its high negative charge, and generation of active drug outside the cytoplasm would not be effective due to its own intrinsic charge. Therefore, the nanodrug can only give rise to nucleic acid methylation if it is internalized into the cytoplasm of recipient cells. The results in Fig. 7 show that drug uptake most likely follows receptor-mediated endocytosis and possibly pinocytotic pathways of the conjugates P/PEG(2%)/LLL(40%)/TMZH(17%)/HuTfR mAb(0.25%) and P/PEG(2%)/LLL(40%)/TMZH(17%) that were labeled with Alex680. Without releasing from the endosome into the cytoplasm, drug activation would still be ineffective due to the stable vesicle membrane barrier. This explains why conjugate P/PEG(2%)/TMZH(30%) without any endosome disruption unit did not affect cell viability (Fig. 4). Moreover, maturing endosomes undergo acidification, rendering drug activation unlikely, because this requires neutral or higher pH. If the nanodrug carries the membrane-disrupting LLL device, as in the case of the above conjugates, it could enter the cytoplasm, and there, by virtue of physiological pH, the prodrug could be converted into its active form and methylate DNA.

To satisfy the above mechanism, we have synthesized the nanodrug carrying targeting TfR antibodies, endosome disruption unit, and the prodrug. The results in Figs. 4 and 6 suggest the delivery and prodrug activation follow the anticipated mechanism. It was noted, however, that the effect of the targeting HuTfR mAb was too potent as observed in the case of human glioma U87MG cells, whereas in human breast cancer cells MDA MB-468 (Fig. 6), the antibody effect was not significant compared with the conjugates without it. This could be accounted for if levels of TfR expression were lower for MDA MB-468 than for U87MG cells. Nevertheless, a significant reduction of viability is seen in the presence of the endosome escape unit LLL for all cell lines shown in Figs. 4 and 6. This is in agreement with the assumed stringent requirement for endosome escape in the prodrug delivery mechanism.

Whereas glioma U87MG cells responded to treatment with free TMZ, cell viability of glioma T98G and breast cancer MDA-MB-231 and MDA-MB-468 cells did not change. These cell lines are known to be TMZ resistant (32–34). In the case of T98G cells, resistance has been referred to overproduction of O6-methyl guanine methyltransferase (MGMT) (32); that of MDA-MB-231 cells has been associated with unbalanced expression of DNA glycosylase and DNA polymerase expression (36), and the mechanism of resistance is not known for MDA-MB-468 cells. If indeed the lack of response to free TMZ for T98G, MDA-MB-231 and MDA-MB-468 in Fig. 4 referred to TMZ resistance, the observed significant decrease of cell viability (Figs. 4 and 6) suggested that the nanoconjugates P/PEG(2%)/LLL(40%)/TMZH(17%), P/LLL(40%)/PEG(2%)/TMZH(17%)/HuTfR mAb(0.25%) and P/LLL(40%)/PEG(2%)/TMZH(17%)/IgG(0.25%) had the ability to overcome the resistance. On the basis of their unique results, conjugates P/PEG(2%)/LLL(40%)/TMZH(17%) and P/LLL(40%)/PEG(2%)/TMZH(17%)/HuTfR mAb (0.25%) were designed as lead compounds with potential for treatment of glial tumors *in vivo*.

Our drug delivery system offers a biodegradable, nontoxic, and non-immunogenic scaffold obtained from a biological source, thus opening an avenue for drug delivery without the danger of liver storage disease. Conjugation of TMZH to this platform has been challenging because of the sensitivity of the prodrug to neutral and alkaline pH. Nonetheless, syntheses of TMZ nanodrugs have been worked out to be readily achievable and highly reproducible. The solution properties, such as solubility and absence of aggregation, size in the nanometer range, and slightly negative zeta potential, are favorable for drug delivery (37,38). One of our lead conjugates contains PEG_{5000}, which is known to minimize enzymatic nanodrug degradation and clearance by the reticulo-endothelial system (39). The nanodrugs are stable in human plasma over several hours, and the range of half-life for active drug formation has increased several-fold over that of free TMZ by conjugation to the PMLA platform. The increased half-life of conjugated TMZ would favor an efficient delivery of functional prodrug *in vivo*. On the basis of *in vitro* experimental data, the following *in vivo* scenario is likely: After I.V. application, the nanodrug will be accumulated in the interstitial space of malignant glioma by EPR effect (19) and/or active mAb targeting of overexpressed TfR on vascular endothelium next to the tumor (21). From the interstitium, the nanodrug will enter the endosomal system of tumor cells and become activated in the cytoplasm after endosomal escape. Accumulation in the tumor by EPR effect and, especially, active mAb targeting would provide necessary efficiency of tumor treatment with minimal side effects for healthy tissue.

CONCLUSIONS

For the purpose of targeting TMZ to human glioma, TMZH was conjugated to PMLA platform, which was equipped with anti-human TfR antibodies for tumor cell targeting by receptor-mediated endocytosis and pH-dependent LLL for endosome escape. Half-life of TMZ was significantly enhanced, about 3-4 times, after conjugation with polymer. The lead compounds P/PEG(2%)/LLL(40%)/TMZH(17%)/HuTfR mAb(0.25%) and P/LLL(40%)/TMZH(17%) showed significant reduction in tumor cell viability of both human glioma and human breast cancer cell lines. Cell

viability was significantly reduced in cases of TMZ-resistant cell lines where free TMZ had no effect. The stage is now set for *in vivo* treatment.

ACKNOWLEDGEMENTS

We greatly acknowledge financial support by NIH R01 CA123495 and grant from the Department of Neurosurgery at Cedars-Sinai Medical Center. Dr. Reinhard Sterner, Institut für Biophysik und physikalische Biochemie der Universität Regensburg, Regensburg, Germany supported the production of polymalic acid.

REFERENCES

1. Louis DN, Ohgaki H, Wiestler OD, Cavenee WK, Burger PC, Jouvet A, *et al.* The 2007 WHO classification of tumours of the central nervous system. Acta Neuropathol. 2007;114:97–109.
2. 2009 CBTRUS Statistical Report: Primary Brain and Central Nervous System Tumors Diagnosed in the United States in 2004–2005. http://www.cbtrus.org/reports/2009-NPCR-04-05/CBTRUS-NPCR2004-2005-Report-.pdf (accessed 11/17/09).
3. Asthagiri AR, Pouratian N, Sherman J, Ahmed G, Shaffrey ME. Advances in brain tumor surgery. Neurol Clin. 2007;25:975–1003.
4. Stummer W, Pichlmeier U, Meinel T, Wiestler OD, Zanella F, Reulen HJ. Fluorescence-guided surgery with 5-aminolevulinic acid for resection of malignant glioma: a randomised controlled multicentre phase III trial. Lancet Oncol. 2006;7:392–401.
5. Lacroix M, Abi-Said D, Fourney DR, Gokaslan ZL, Shi W, DeMonte F, *et al.* A multivariate analysis of 416 patients with glioblastoma multiforme: prognosis, extent of resection, and survival. J Neurosurg. 2001;95:190–8.
6. Arrowsmith J, Jennings SA, Langnel DA, Wheelhouse RT, Stevens MF. Antitumour imidazotetrazines. Part 39 synthesis of bis(imidazotetrazine)s with saturated spacer groups. J Chem Soc Perkin Trans 1. 2000;24:4432–8.
7. Stupp R, Mason WP, van den Bent MJ, Weller M, Fisher B, Taphoorn MJ, *et al.* Radiotherapy plus concomitant and adjuvant temozolomide for glioblastoma. N Engl J Med. 2005;352:987–96.
8. Auger N, Thillet J, Wanherdrick K, Idbaih A, Legrier ME, Dutrillaux B, *et al.* Genetic alterations associated with acquired temozolomide resistance in SNB-19, a human glioma cell line. Mol Cancer Ther. 2006;5:2182–92.
9. Chen CC, Kahle KT, Ng K, Nitta M, Andrea AD. Of escherichia coli and man: understanding glioma resistance to temozolomide therapy. In: Meir EG, editor. CNS Cancer. Atlanta: Humana; 2009. p. 679–711.
10. Kitange GJ, Carlson BL, Schroeder MA, Grogan PT, Lamont JD, Decker PA, *et al.* Induction of MGMT expression is associated with temozolomide resistance in glioblastoma xenografts. Neuro Oncol. 2009;11:281–91.
11. Satchi-Fainaro R, Puder M, Davies JW, Tran HT, Sampson DA, Greene AK, *et al.* Targeting angiogenesis with a conjugate of HPMA copolymer and TNP-470. Nat Med. 2004;10:255–61.
12. Duncan R. The dawning era of polymer therapeutics. Nat Rev Drug Discov. 2003;2:347–60.
13. Vinogradov SV, Batrakova EV, Li S, Kabanov AV. Mixed polymer micelles of amphiphilic and cationic copolymers for delivery of antisense oligonucleotides. J Drug Target. 2004;12:517–26.
14. Kabanov AV, Batrakova EV, Sriadibhatla S, Yang Z, Kelly DL, Alakov VY. Polymer genomics: shifting the gene and drug delivery paradigms. J Control Release. 2005;101:259–71.
15. Peer D, Karp JM, Hong S, Farokhzad OC, Margalit R, Langer R. Nanocarriers as an emerging platform for cancer therapy. Nat Nanotechnol. 2007;2:751–60.
16. Ferrari M. Cancer nanotechnology: opportunities and challenges. Nat Rev Cancer. 2005;5:161–71.
17. Nori A, Kopecek J. Intracellular targeting of polymer-bound drugs for cancer chemotherapy. Adv Drug Deliv Rev. 2005;57:609–36.
18. Duncan R, Vicent MJ, Greco F, Nicholson RI. Polymer-drug conjugates: towards a novel approach for the treatment of endrocine-related cancer. Endocr Relat Cancer. 2005;12:S189–99.
19. Maeda H, Fang J, Inutsuka T, Kitamoto Y. Vascular permeability enhancement in solid tumor: various factors, mechanisms involved and its implications. Int Immunopharmacol. 2003;3:319–28.
20. Fujita M, Lee BS, Khazenzon NM, Penichet ML, Wawrowsky KA, Patil R, *et al.* Brain tumor tandem targeting using a combination of monoclonal antibodies attached to biopoly(β-L-malic acid). J Control Release. 2007;122:356–63.
21. Lee BS, Fujita M, Khazenzon NM, Wawrowsky KA, Wachsmann-Hogiu S, Farkas DL, *et al.* Polycefin, a new prototype of a multifunctional nanoconjugate based on poly(β-L-malic acid) for drug delivery. Bioconjug Chem. 2006;17:317–26.
22. Segal E, Satchi-Fainaro R. Design and development of polymer conjugates as anti-angiogenic agents. Adv Drug Deliv Rev. 2009;61:1159–76.
23. Brem S, Tyler B, Li K, Pradilla G, Legnani F, Caplan J, *et al.* Local delivery of temozolomide by biodegradable polymers is superior to oral administration in a rodent glioma model. Cancer Chemother Pharmacol. 2007;60:643–50.
24. Akbar U, Jones T, Winestone J, Michael M, Shukla A, Sun Y, *et al.* Delivery of temozolomide to the tumor bed via biodegradable gel matrices in a novel model of intracranial glioma with resection. J Neurooncol. 2009;94:203–12.
25. Zhao LX, Wang JL, Dai XP, Wang YF, Ji ZZ. Synthesis and antitumour activities of 3-substituted 4-oxo-3 H-imidazo[5, 1-d] [1, 2, 3, 5] tetrazine-8-carboxylic acids and their derivatives. Chin J Med Chem. 2001;11:263–9.
26. Holler E. Poly(malic acid) from natural sources. In: Cheremisinoff NP, editor. Handbook of engineering polymeric materials. New York: Marcel Dekker; 1997. p. 93–103.
27. Carlsson J, Drevin H, Axen R. Protein thiolation and reversible protein-protein conjugation. N-Succinimidyl 3-(2-pyridyldithio) propionate, a new heterobifunctional reagent. Biochem J. 1978;173:723–37.
28. Ljubimova JY, Fujita M, Ljubimov AV, Torchilin VP, Black KL, Holler E. Poly(malic acid) nanoconjugates containing various antibodies and oligonucleotides for multitargeting drug delivery. Nanomedicine. 2008;3:247–65.
29. I. O. f.S. (ISO). Methods for Determination of Particle Size Distribution Part 8: Photon Correlation Spectroscopy, International Standard ISO 13321, 1996.
30. Hiemenz PC. Light scattering by polymer solutions. In: Hiemenz PC, editor. Polymer chemistry: The basic concepts. New York: Marcel Decker; 1984. p. 659–61.
31. Fu FN, Singh BR. Calcein permeability of liposomes mediated by type A botulinum neurotoxin and its light and heavy chains. J Protein Chem. 1999;18:701–7.
32. Mosmann TJ. Rapid colorimetric assays for cellular growth and survival: application to proliferation and cytotoxicity assays. Immunol Methods. 1983;65:55–63.

33. Friedman HS, Kerby T, Calvert H. Temozolomide and treatment of malignant glioma. Clin Cancer Res. 2000;6:2585–97.
34. Maeda H, Sawa T, Konno T. Mechanism of tumor-targeted delivery of macromolecular drugs, including the EPR effect in solid tumor and clinical overview of the prototype polymeric drug SMANCS. J Control Release. 2001;74:47–61.
35. Matsumuraand Y, Maeda H. A new concept for macromolecular therapeutics in cancer chemotherapy: mechanism of tumoritropic accumulation of proteins and the antitumor agent smancs. Cancer Res. 1986;46:6387–92.
36. Trivedi RN, Wang XH, Jelezcova E, Goellner EM, Tang JB, Sobol RW. Human methyl purine DNA glycosylase and DNA polymerase β expression collectively predict sensitivity to temozolomide. Mol Pharmacol. 2008;74:505–16.
37. Nel AE, Madler L, Velegol D, Xia T, Hoek EM, Somasundaran P, *et al.* Understanding biophysicochemical interactions at the nano-bio interface. Nat Mater. 2009;8:543–57.
38. Lorenz MR, Holzapfel V, Musyanovych A, Nothelfer K, Walther P, Frank H, *et al.* Uptake of functionalized, fluorescent-labeled polymeric particles in different cell lines and stem cells. Biomaterials. 2006;27:2820–8.
39. Owens DE, Peppas NA. Opsonization, biodistribution, and pharmacokinetics of polymeric nanoparticles. Int J Pharm. 2006; 307:93–102.